Biorthogonal Pulse Position Modulation for Time-Hopping Multiple Access UWB Communications

Hao Zhang and T. Aaron Gulliver, *Senior Member, IEEE*

***Abstract*—In this paper, we propose a new modulation scheme called biorthogonal pulse position modulation (BPPM) for ultra-wideband (UWB) communication systems. A set of $N = 2^{k+1}$ BPPM signals are constructed from 2^k orthogonal PPM signals by including the antipodal version of the orthogonal PPM signals. The channel capacity of BPPM is determined for a time-hopping multiple access UWB communication system. The error probability and performance bounds are derived for a multiuser environment. It is shown that N-ary BPPM has better performance than N-ary PPM with the same throughput and half the computational complexity.**

***Index Terms*—Information rates, pulse position modulation, spread spectrum communication, ultra-wideband (UWB) communications.**

I. Introduction

An ULTRA-WIDEBAND (UWB) [1] communication system transmits information using ultra-short impulses which spread the energy of the signal typically from near dc to several gigahertz. Unlike conventional communication systems, UWB systems operate at baseband, and thus involve no intermediate frequency and no carrier synchronization. UWB theoretically promises a very high data rate by employing a large signal bandwidth. However, power spectrum density limitations such as FCC Part 15 rules limit the system capability. In particular, UWB systems under FCC Part 15 rules provide reliable communications only over small to medium distances. Typically, pulse amplitude modulation (PAM), pulse position modulation (PPM), or on/off keying (OOK) modulation is employed. PPM modulation uses the precise collocation of the impulses in time to convey information, while PAM and OOK use amplitude for this purpose. UWB systems with PAM and PPM modulation have been extensively investigated. In [1], [2], [5], and [6], a time-hopping multiple-access scheme for UWB systems with PPM was considered. A PPM UWB system over an additive white Gaussian noise (AWGN) channel was considered from the capacity perspective (subject to FCC Part 15 rules) in [3], [4]. The performance of a PAM UWB system with a Rake receiver was investigated in [7], [9] for an indoor wireless channel with multipath interference. An all-digital multiple access scheme based upon PAM and TDM was proposed in [8]. The construction of equal energy N-orthogonal time-shift-modulated codes were described in [11]. In [12], the effective capacity of a pulse-position hopping code division multiple access (CDMA) system with OOK modulation was analyzed.

In this paper, we propose a new modulation scheme, called biorthogonal pulse position modulation. A set of $N = 2^{k+1}$ biorthogonal pulse position modulation (BPPM) signals are constructed from 2^k orthogonal PPM signals by including the antipodal version of the orthogonal PPM signals. It is shown that the proposed BPPM has better performance and less complexity than PPM with the same throughput. Note that in the rest of the paper, PPM denotes classical orthogonal PPM unless otherwise specified. This paper presents the capacity and error probability of an N-ary BPPM UWB system, as well as the multiple-access capacity subject to specific waveforms, from a signal-to-noise ratio (SNR) perspective. Differentiated pulses with a Gaussian or Manchester pulse shape are considered. This analysis can easily be extended to other waveforms.

The rest of the paper is organized as follows. In Section II, the system model and construction of the time-hopping BPPM UWB signal are described. Section III presents the capacity and error probability analysis of the BPPM UWB system over an AWGN channel for a single user. The relationship between the reliable communication distance and channel capacity subject to FCC Part 15 rules is demonstrated. The exact error probability for N-ary BPPM is presented, and a simple upper bound on the probability of error is derived. The multiple access capacity and error probability of a BPPM UWB system are derived in Section IV. Section V presents numerical results on the system performance and capacity, and finally some conclusions are given in Section VI.

II. Signal Construction and the System Model

Constructed from 2^k orthogonal PPM signals, a set of $N = 2^{k+1}$ BPPM signals include the antipodal version of the orthogonal PPM signals. An N-ary BPPM signal $\mathbf{s}_{mn}$ is defined as an $N/2$-dimensional vector with nonzero value in the nth dimension

$$\mathbf{s}_{mn} = [0, \ldots, 0, A_m\sqrt{E_g}, 0, \ldots, 0] \tag{1}$$

where N is an even integer and $N > 0, 1 \le n \le N/2, m = 1$ or 2, $A_1 = 1$, $A_2 = -1$, and E_g is the average energy of the signal.

Manuscript received June 16, 2003; revised January 5, 2004. The editor coordinating the review of this paper and approving it for publication is Z. Tian.

The authors are with the Department of Electrical and Computer Engineering, University of Victoria, Victoria, BC V8W 3P6 Canada (e-mail: hzhang@ece.uvic.ca; agullive@ece.uvic.ca).

Digital Object Identifier 10.1109/TWC.2005.846969

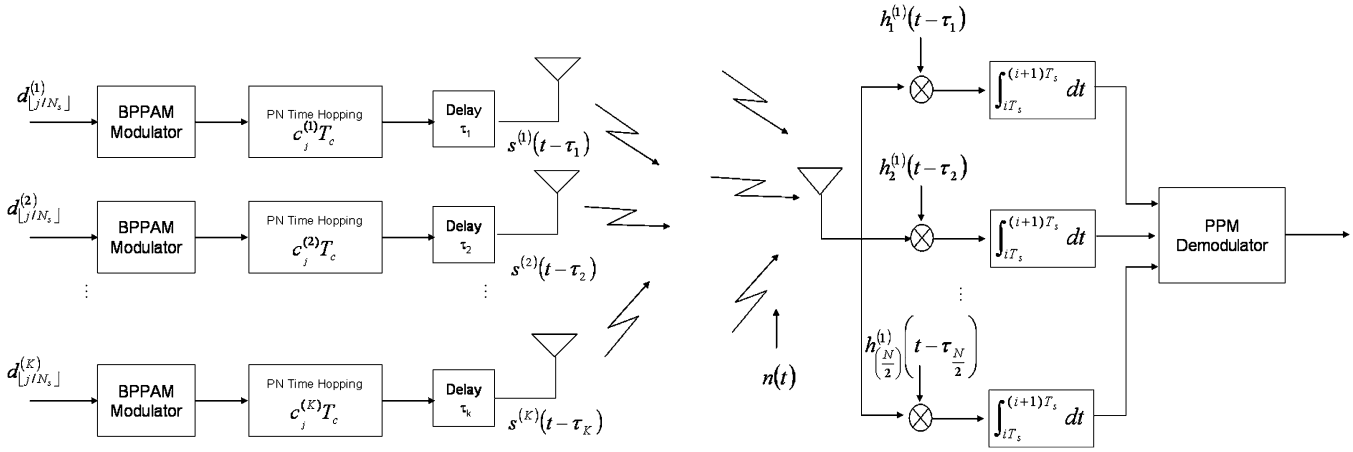

Fig. 1. System model of a time-hopping multiple-access N-ary biorthogonal PPM UWB system.

A typical time hopping format for the signal of the kth user in an UWB system is given by [10]

$$s^{(k)}(t) = \sum_{j=-\infty}^{\infty} A^{(k)}_{d_{\lfloor j/N_s \rfloor}} q\left(t - jT_f - c_j^{(k)} T_c - \delta_{d^{(k)}_{\lfloor j/N_s \rfloor}}\right) \tag{2}$$

where $q(t)$ represents the transmitted impulse waveform that nominally begins at time zero, and the quantities associated with (k) are transmitter dependent. T_f is the frame time, which is typically a hundred to a thousand times the impulse width resulting in a signal with very low duty cycle. A data symbol is transmitted using N_s UWB pulses. Each frame is divided into N_h time slots with duration T_c. The pulse shift pattern $c_j^{(k)}$, $0 \le c_j^{(k)} \le N_h$ (also called time-hopping sequence), is pseudorandom, which provides an additional shift in order to avoid catastrophic collisions due to multiple access interference. The sequence d is the N-ary data stream generated by the kth source after channel coding, $\delta_{d^{(k)}_{\lfloor j/N_s \rfloor}}$ is the additional modulation time shift utilized for PPM determined by the input data d, and $A^{(k)}_{d_{\lfloor j/N_s \rfloor}}$ is the signal amplitude which depends on d. If $N_s > 1$ a repetition code is introduced, i.e., N_s pulses are used for the transmission of the same information symbol.

The received signal can be modeled as the derivative of the transmitted pulses assuming propagation in free space [1]

$$\begin{aligned} r(t) &= \sum_{k=1}^{K} \left(s^{(k)}(t-\tau_k)\right)' + w(t) \\ &= \sum_{k=1}^{K} \sum_{j=-\infty}^{\infty} A^{(k)}_{d_{\lfloor j/N_s \rfloor}} \\ &\quad \times p\left(t - jT_f - c_j^{(k)} T_c - \delta_{d^{(k)}_{\lfloor j/N_s \rfloor}}\right) + w(t)' \end{aligned} \tag{3}$$

where $w(t)$ is AWGN noise with power density $N_0/2$, τ_k is the propagation delay for the kth user and $p(t)$ is the received pulse waveform. If only one user is present, the optimal receiver is an $N/2$-ary correlation receiver followed by a detector. When more than one link is active in the multiple-access system, the optimal receiver has a complex structure that takes advantage of all receiver knowledge regarding the characteristics of the multiple-access interference (MAI) [4]. However, for simplicity, an $N/2$-ary correlation receiver is typically used even when there is more than one active user. Fig. 1 shows the structure of the correlation receiver of the proposed N-ary BPPM UWB system.

III. Single User Capacity and Error Probability

With a single user active in the system, AWGN is the only source of signal degradation. For simplicity, we further assume that $\delta \ge T_p$, where T_p is the pulse duration, i.e., the N-ary BPPM signal constellation consists of a set of $N/2$-orthogonal signals with equal energy, plus the antipodal version of these signals. Then the analysis in [17], [18] for the capacity of modulated channels for PPM and PAM, and the error probability analysis in [16] for PPM, PAM, and biorthogonal signals, can be applied to the proposed BPPM system.

A. Channel Capacity for N-ary BPPM Over AWGN Channels

The Shannon capacity $C = W \log_2(1 + \mathrm{SNR})$, where SNR is the signal-to-noise ratio and W is the channel bandwidth, predicts the channel capacity C for an AWGN channel with continuous-valued inputs and outputs. However, a channel with N-ary BPPM modulation has discrete-valued inputs and continuous-valued outputs, which imposes an additional constraint on the capacity calculation. Let $\mathbf{s}_{mn}$ be the encoded $N/2$-dimensional BPPM signal vector input to the channel, and $\mathbf{r}$ be the channel output vector corrupted by an AWGN noise vector $\mathbf{w}$, which has zero mean and variance $\sigma^2 = (1/2)N_0/z$ in each real dimension. The vector representation of (3) for a single user is

$$\mathbf{r} = \mathbf{s}_{mn} + \mathbf{w}. \tag{4}$$

From [13], [17], [18], the channel capacity with input signals restricted to an equiprobable N-ary BPPM constellation and no restriction on the channel output, is given by

$$\begin{aligned} C = \log_2 N - \frac{1}{N} \sum_{m=1}^{2} \sum_{n=1}^{N/2} \int \int_r p(r|s_{mn}) \\ \times \log_2 \left(\frac{\sum_{p=1}^{2} \sum_{q=1}^{N/2} p(r|s_{pq})}{p(r|s_{mn})} \right) dr \end{aligned} \tag{5}$$

where $\mathbf{r} = (r_1, \ldots, r_{N/2})$ is the $N/2$-dimensional received vector, $r_i = w_i$ for $i \neq n$ and $r_n = A_m\sqrt{E_g} + w_n$. $\mathbf{s}_{mn}$ is the input BPPM signal defined in (1). The received signal $\mathbf{r}$ will have a $N/2$-dimensional joint Gaussian distribution conditioned on $\mathbf{s}_{mn}$, with probability density function (PDF)

$$p(\mathbf{r}|\mathbf{s}_{mn}) = \left(\frac{1}{2\pi\sigma^2}\right)^{N/4} \times \left(\prod_{\substack{i=1 \\ i\neq n}}^{N/2} e^{\left(-r_i^2/2\sigma^2\right)}\right) e^{-\left((r_n - A_m\sqrt{E_g})^2/2\sigma^2\right)}. \quad (6)$$

The channel capacity for an N-ary BPPM UWB system over an AWGN channel can then be written from (5) as (7), shown at the bottom of the page.

B. Capacity of an N-ary BPPM UWB System Under FCC Part 15 Rules

Due to the possible interference to other communication systems by the UWB impulses, UWB transmissions are currently only allowed on an unlicensed basis subject to FCC Part 15 rules which restricts the field strength level to $E = 500$ microvolts/mter/MHz at a distance of 3 m. This gives a transmitted power constraint for an UWB system with a 1 GHz bandwidth of $P_t \leq -11$ dBm. The following relationship is obtained using a common link budget model [3], [4]

$$\frac{\gamma}{G} \leq -11 \text{ dBm} - N_{\text{thermal}} - F - 10\log\frac{(4\pi d)^n}{\lambda} \quad (8)$$

where $G = N_s T_f W_p$ is the equivalent processing gain, W_p is the bandwidth of the UWB impulse related to the pulse duration T_p, F is the noise figure, N_{thermal} is the thermal noise floor, calculated as the product of Boltzman's constant, room temperature (typically 300 K), noise figure and bandwidth, λ is the wavelength corresponding to the center frequency of the pulse, and n is the path loss exponent. It is easily shown that the maximum reliable communication distance is determined primarily by the signal to noise ratio γ. Based upon (7) and (8), the maximum distance for reliable transmission can be calculated. The relationship between system capacity and communication range will be demonstrated in Section V.

C. Error Probability of N-ary BPPM Over an AWGN Channel

For N-ary biorthogonal signals, the optimal receiver consists of a parallel bank of N crosscorrelators. However, the biorthogonal design allows us to obviate the correlators for the inverse of the $N/2$ orthogonal signals without affecting performance. Thus the receiver has a parallel bank of $N/2$ crosscorrelators as illustrated in Fig. 1. Let $\mathbf{h}_j$, $1 \leq j \leq N/2$, denote the jth basis signal vector, which is the vector representation of the basis function $h_j(t)$ shown in Fig. 1, defined as

$$\mathbf{h}_j = [0, \ldots, 0, 1, 0, \ldots, 0] \quad (9)$$

where the nonzero value 1 is in the jth dimension. Assuming $\mathbf{s}_{mn}$ was sent, the optimum detector makes a decision on $\mathbf{s}_{mn}$ in favor of the signal corresponding to the crosscorrelator with the minimum Euclidean distance

$$C(\mathbf{r}, \mathbf{h}_j) = \mathbf{r} \cdot \mathbf{h}_j = \sum_{k=1}^{N/2} r_k h_{jk}, \quad j = 1, 2, \ldots, \frac{N}{2} \quad (10)$$

where

$$\begin{aligned} C(\mathbf{r}, \mathbf{h}_j) &= w_j, \quad j \neq n \\ C(\mathbf{r}, \mathbf{h}_n) &= A_m\sqrt{E_g} + w_n. \end{aligned} \quad (11)$$

Thus with the optimum detector and $N_{\mathbf{s}} = 1$, the demodulated signal $\hat{\boldsymbol{s}}$ can be given as

$$\begin{aligned} \hat{\boldsymbol{s}} &= \arg\min_{s_{ij}} \|C(\mathbf{r}, \mathbf{h}_j) - A_i\sqrt{E_g}\| \\ & i = 1, 2 \text{ and } j = 1, 2, \ldots, \frac{N}{2}. \end{aligned} \quad (12)$$

The receiver structure can be simplified to facilitate the error probability and union bound analysis. Assuming $\mathbf{s}_{mn}$ was sent, the optimum detector decides on the nonzero dimension of $\mathbf{s}_{mn}$, i.e., n, in favor of the dimension corresponding to the largest magnitude of the crosscorrelators given in (10), and the sign of this magnitude is used to decide which of the two possible amplitudes, i.e., m, has been transmitted. Using standard techniques [16], the average probability of a correct decision is given by

$$P_c = \int_0^\infty \left(\frac{1}{\sqrt{2\pi}} \int_{-r_1/\sqrt{N_0/2}}^{r_1/\sqrt{N_0/2}} e^{-x^2/2} dx\right)^{N/2-1} p(r_1) dr_1 \quad (13)$$

where

$$p(r_1) = \frac{1}{\sqrt{\pi N_0}} \exp\left(-\frac{(r_1 - \sqrt{E_g})^2}{N_0}\right). \quad (14)$$

Finally, the probability of a symbol error for N-ary BPPM is

$$P_N = 1 - P_c. \quad (15)$$

As given in [19], [20], the performance of a binary time hopping PPM system with a single user is $P_{2PPM} = Q\left(\sqrt{(E_g/N_0)(1 - \gamma(\delta))}\right)$, where $\gamma(\cdot)$ is the autocorrelation function of the received waveform. For binary BPPM,

$$C = \log_2 N - \frac{1}{N} \times \sum_{m=1}^{2}\sum_{n=1}^{N/2} E_{r|s_{mn}}\left[\log_2\left(\sum_{p=1}^{2}\sum_{q=1}^{N/2} \exp\left(-\frac{r_n^2 - r_q^2 + \left(r_q - A_p\sqrt{E_g}\right)^2 - \left(r_n - A_m\sqrt{E_g}\right)^2}{2\sigma^2}\right)\right)\right] \text{ bits / channel use} \quad (7)$$

i.e., $N = 2$, we have $P_{2BPPM} = Q\left(\sqrt{2E_g/N_0}\right)$ from (15). Obviously, the proposed orthogonal binary BPPM performs better than binary time hopping PPM since $-1 \leq \gamma(\delta) \leq 1$. Note that the computational complexity of binary BPPM is only about half that of binary PPM.

D. A Union Bound on the Probability of Error

Since the probability of error expressions given by (13) and (15) are complex, and must be evaluated via numerical integration, we now derive a simple upper bound on the probability of a symbol error. Assuming an equiprobable N-ary BPPM constellation, an upper bound on the error probability of a BPPM signal over an AWGN channel can be obtained using the simplified receiver structure from subsection C

$$\begin{aligned} P_{N|s_{mn}} &= P_{N|s_{1n}} \\ &\leq P\left(\left(\bigcup_{\substack{j=1 \\ j\neq n}}^{N/2} |C(\mathbf{r},\mathbf{h}_j)| > |C(\mathbf{r},\mathbf{h}_n)|\right)\right. \\ &\qquad \left.\times \bigcup (C(\mathbf{r},\mathbf{h}_n) < 0)\right). \end{aligned} \tag{16}$$

The right-hand term of (16) is then upper-bounded by the union bound of the $N/2$ events, i.e.,

$$\begin{aligned} P_{N|s_{mn}} &\leq P\left(\left(\bigcup_{\substack{j=1 \\ j\neq n}}^{N/2} |C(\mathbf{r},\mathbf{h}_j)| > |C(\mathbf{r},\mathbf{h}_n)|\right)\right. \\ &\qquad \left.\times \bigcup C(\mathbf{r},\mathbf{h}_n) < 0\right) \\ &\leq \sum_{\substack{j=1 \\ j\neq n}}^{N/2} P\left(|C(\mathbf{r},\mathbf{h}_j)| > |C(\mathbf{r},\mathbf{h}_n)|\right) \\ &\quad + P\left(\sqrt{E_g} + w_n < 0\right) \\ &= \left[\left(\frac{N}{2} - 1\right) P(|C(\mathbf{r},\mathbf{h}_j)| > |C(\mathbf{r},\mathbf{h}_n)|)\right. \\ &\qquad \left. + P\left(\sqrt{E_g} + w_n < 0\right)\right]\Big|_{\forall\, j\neq n}. \end{aligned} \tag{17}$$

Given $C(\mathbf{r},\mathbf{h}_j)$, $j = 1,\ldots,N/2$, as in (11), it can be shown that

$$P(|C(\mathbf{r},\mathbf{h}_j)| > |C(\mathbf{r},\mathbf{h}_n)|)\big|_{s_{1n}, j\neq n} < \frac{\sqrt{2}}{2} e^{-(E_g/2N_0)} \tag{18}$$

and

$$P\left(\sqrt{E_g} + w_n < 0\right)\Big|_{s_{1n}} = Q\left(\sqrt{\frac{2E_g}{N_0}}\right). \tag{19}$$

Assuming all BPPM signals are equally likely *a priori*, an upper bound on the average probability of symbol error for N-ary BPPM is given by

$$P_N < \left(\frac{N}{2} - 1\right)\frac{\sqrt{2}}{2} e^{-(E_g/2N_0)} + Q\left(\sqrt{\frac{2E_g}{N_0}}\right). \tag{20}$$

To further simplify this bound, we employ

$$Q(x) < e^{-(x^2/2)} \tag{21}$$

to obtain

$$\begin{aligned} P_N &< \left(\frac{N}{2} - 1\right)\frac{\sqrt{2}}{2} e^{-(E_g/2N_0)} + e^{-(E_g/2N_0)} \\ &< \frac{N}{2} e^{-(E_g/2N_0)}. \end{aligned} \tag{22}$$

From [16], the N-ary PPM signals are mutually equidistant, i.e., geometrically the distance between any pair of signal vectors is $\sqrt{2E_s}$, while for biorthogonal PPM signals, the distance between any pair of signal vector is either $\sqrt{2E_s}$ or $2\sqrt{E_s}$. Hence from the signal space perspective, N-ary biorthogonal PPM signals have better performance than N-ary PPM signals. Using the union bound given in [16] for PPM, we obtain another upper bound for N-ary BPPM

$$P_N < P_{N,PPM} < (N-1)Q\left(\sqrt{\frac{E_g}{N_0}}\right). \tag{23}$$

It will be shown in Section V that (23) is a tighter upper bound than (22). Note that for the same throughput, biorthogonal signalling only requires half the number of crosscorrelators required by PPM, and thus has only about half the computational complexity with better performance. Therefore, N-ary BPPM, i.e., biorthogonal signalling, is an attractive choice for UWB communication systems.

IV. Multiple Access Capacity and Error Probability

With more than one user active in the system, MAI is a factor limiting performance and capacity, especially for a large number of users. As shown in [13], the net effect of the multiple-access interference produced by the undesired users at the output of the desired user's correlation receiver can be modeled as a zero-mean Gaussian random variable, if the number of users is large [16]. Assuming that $\delta \geq T_p$,, i.e., the N-ary BPPM signal is an orthogonal signal with $N/2$ dimensions, the capacity and error probability analysis given in Section III for a single user can be extended to multiple-access systems.

A. MAI Model

As given in (3), the received signal is modeled as

$$r(t) = \sum_{k=1}^{K} \left(s^{(k)}(t - \tau_k)\right)' + n(t). \tag{24}$$

To evaluate the average SNR, we make the following assumptions.

a) $s^{(k)}(t-\tau_k)$, for $k = 1, 2, \ldots, K$, where K is the number of active users, and the noise $n(t)$ is assumed to be independent.
b) The time-hopping sequences $c_j^{(k)}$ are assumed to be independent, identically distributed (i.i.d) random variables uniformly distributed over the time interval $[0, N_h]$.
c) All N-ary BPPM signals are equally likely *a priori*.

d) The time delay τ_k is assumed to be i.i.d and uniformly distributed over $[0, T_f]$.
e) Perfect synchronization is assumed at the receiver, i.e., τ_k is known at the receiver.

We will show that we may assume that each information symbol only uses a single UWB pulse, i.e., $N_s = 1$ later in this section.

Without loss of generality, we assume the desired user is that corresponding to $k = 1$. The basis functions of the N crosscorrelators of the correlation receiver for user 1 are

$$h_i^{(1)} = p(t - \delta_i - \tau_1), \quad i = 1, \ldots, N. \tag{25}$$

The output of each crosscorrelator in the sample period $[lN_sT_f\ (l+1)N_sT_f]$, where l is an integer, is

$$\begin{aligned}\hat{r}_i = &\sum_{j=lN_s+1}^{(l+1)N_s} \int_{(j-1)T_f}^{jT_f} r(t) h_i^{(1)} \\ &\times \left(t - jT_f - c_j^{(k)} T_c - \delta_{d^{(k)}_{\lfloor j/N_s \rfloor}}\right) dt \\ &i = 1, \ldots, N.\end{aligned} \tag{26}$$

Assuming BPPM signal $\mathbf{s}_{mn}$ is transmitted by user 1, (26) can be written as

$$\hat{r}_i = \begin{cases} N_s A_d^{(1)} \sqrt{E_g} + W_{\mathrm{MAI}} + W & i = n \\ W_{\mathrm{MAI}} + W & i \neq n \end{cases} \tag{27}$$

where

$$\begin{aligned}W_{\mathrm{MAI}} = &\sum_{k=2}^{K} \sum_{j=lN_s+1}^{(l+1)N_s} \int_{(j-1)T_f}^{jT_f} A^{(k)}_{d_{\lfloor j/N_s \rfloor}} \\ &\times p\left(t - jT_f - c_j^{(k)} T_c - \delta_{d^{(k)}_{\lfloor j/N_s \rfloor}} - \tau_k\right) \\ &\times p\left(t - \delta_i - \tau_1 - jT_f - c_j^{(k)} T_c\right) dt\end{aligned} \tag{28}$$

is the MAI component and

$$W = \sum_{j=lN_s+1}^{(l+1)N_s} \int_{(j-1)T_f}^{jT_f} n(t) p\left(t - \delta_i - \tau_1 - jT_f - c_j^{(k)} T_c\right) dt \tag{29}$$

is the AWGN component. By defining the autocorrelation function of $w(t)$ as

$$\gamma(\Delta) = \int_0^{T_f} p(t) p(t - \Delta) dt \tag{30}$$

(28) can be written as

$$W_{\mathrm{MAI}} = \sum_{j=1}^{N_s} \sum_{k=2}^{K} A_d^{(k)} \gamma\left(\Delta_j^{(k)}\right) \tag{31}$$

where $\Delta_j^{(k)} = \left(c_j^{(1)} - c_j^{(k)}\right) T_c - \left(\delta_i^{(1)} - \delta d^{(k)}_{\lfloor j/N_s \rfloor}\right) - (\tau_1 - \tau_k)$, is the time difference between user 1 and user k. Under the assumptions listed above, Δ can be modeled as a random variable uniformly distributed over $[-T_f, T_f]$. As in [1], [10], and [20], the MAI is modeled as a Gaussian random process for the multiuser environment. Note that $N_s \gg 1$ justifies the Gaussian approximation even for a small number of users as illustrated in [20]. With the Gaussian approximation [1], [10], [20], we require the mean and variance of (27) to characterize the output of the crosscorrelators.

It is easy to show that the AWGN component has mean zero and variance $N_sN_0/2$. However, the mean and variance of the MAI component are determined by the specific pulse waveform. In this paper, we consider the received signal pulses to be differentiated pulses with Gaussian or Manchester pulse shape. Therefore, the transmitted pulses are Gaussian pulses or Triangle pulses, respectively. Note that both of these pulses satisfy the relation $\int_{-\infty}^{\infty} p(t)dt = 0$, i.e., no dc value appears in the power spectrum of the pulse. As in [12], the differentiated Gaussian pulse is defined as

$$w_{\mathrm{DGaussian}}(t) = \begin{cases} \frac{\sqrt{8}}{\sqrt[4]{2\pi\lambda^3 T_p^6}} t e^{-\left(t^2/\lambda T_p^2\right)}, & -\frac{T_p}{2} \leq t \leq \frac{T_p}{2} \\ 0, & \text{otherwise} \end{cases} \tag{32}$$

where $\lambda = 0.0815$ is a bandwidth normalization parameter such that 99% of the pulse energy is contained in the range; the Manchester pulse is defined as

$$w_{\mathrm{Manchester}}(t) = \begin{cases} -\sqrt{\frac{1}{T_p}}, & 0 < t < \frac{T_p}{2} \\ \sqrt{\frac{1}{T_p}}, & \frac{T_p}{2} < t < T_p \\ 0, & \text{otherwise.} \end{cases} \tag{33}$$

The autocorrelation functions of the differentiated Gaussian pulse and the Manchester pulse are then

$$\begin{aligned}&\gamma_{\mathrm{DGaussian}}(\Delta) \\ &\quad = \begin{cases} \left(1 - \frac{\Delta^2}{\lambda T_p^2}\right) e^{-\left(\Delta^2/2\lambda T_p^2\right)}, & 0 \leq |t| \leq T_p \\ 0, & \text{otherwise} \end{cases}\end{aligned} \tag{34}$$

and

$$\gamma_{\mathrm{Manchester}}(\Delta) = \begin{cases} \left(1 - \frac{3|\Delta|}{T_p}\right), & 0 \leq |t| \leq \frac{T_p}{2} \\ \left(-1 + \frac{3|\Delta|}{T_p}\right), & \frac{T_p}{2} \leq |t| \leq T_p \\ 0, & \text{otherwise} \end{cases} \tag{35}$$

respectively. Given (34) and (35), we have

$$E[\gamma(\Delta)] = \frac{1}{2T_f} \int_{-T_f}^{T_f} \gamma(\Delta) d\Delta = 0. \tag{36}$$

The mean of W_{MAI} can then be calculated as

$$\begin{aligned}E[W_{\mathrm{MAI}}] &= E\left[\sum_{j=1}^{N_s} \sum_{k=2}^{K} A_d^{(k)} \gamma\left(\Delta_j^{(k)}\right)\right] \\ &= \sum_{j=1}^{N_s} \sum_{k=2}^{K} E\left[A_d^{(k)}\right] E\left[\gamma\left(\Delta_j^{(k)}\right)\right] = 0.\end{aligned} \tag{37}$$

The variance of W_{MAI} for differentiated Gaussian pulses and Manchester pulses is

$$\begin{aligned}Var[W_{\mathrm{MAI}}] &= Var\left[\sum_{j=1}^{N_s} \sum_{k=2}^{K} A_d^{(k)} \gamma\left(\Delta_j^{(k)}\right)\right] \\ &= \sum_{j=1}^{N_s} \sum_{k=2}^{K} E\left[\left(A_d^{(k)}\right)^2\right] \\ &\quad \times E\left[\gamma^2\left(\Delta_j^{(k)}\right)\right].\end{aligned} \tag{38}$$

On the basis that all BPPM signals are equally likely *a priori*, we have

$$\begin{aligned} Var[W_{\mathrm{MAI,DGaussian}}] &= Var\left[\sum_{j=1}^{N_s}\sum_{k=2}^{K} A_d^{(k)}\gamma_{\mathrm{DGaussian}}\left(\Delta_j^{(k)}\right)\right] \\ &= \sum_{j=1}^{N_s}\sum_{k=2}^{K} E\left[\left(A_d^{(k)}\right)^2\right] E\left[\gamma^2_{DGaussian}\left(\Delta_j^{(k)}\right)\right] \\ &= \frac{3\sqrt{\pi\lambda}T_p(K-1)}{8T_f}N_sE_g \end{aligned} \tag{39}$$

for differentiated Gaussian pulses and

$$\begin{aligned} Var[W_{\mathrm{MAI,Manchester}}] &= Var\left[\sum_{j=1}^{N_s}\sum_{k=2}^{K} A_d^{(k)}\gamma_{\mathrm{Manchester}}\left(\Delta_j^{(k)}\right)\right] \\ &= \sum_{j=1}^{N_s}\sum_{k=2}^{K} E\left[\left(A_d^{(k)}\right)^2\right] E\left[\gamma^2_{\mathrm{Manchester}}\left(\Delta_j^{(k)}\right)\right] \\ &= \frac{(K-1)T_p}{6T_f}N_sE_g \end{aligned} \tag{40}$$

for Manchester pulses. By defining the spread ratio $\rho = T_f/T_p$, (39) and (40) can be written as

$$Var[W_{\mathrm{MAI,DGaussian}}] = \frac{3\sqrt{\pi\lambda}(K-1)}{8\rho}N_sE_g \tag{41}$$

and

$$Var[W_{\mathrm{MAI,Manchester}}] = \frac{(K-1)}{6\rho}N_sE_g \tag{42}$$

respectively. Hence the outputs of the crosscorrelators for the receiver of user 1 can be modeled as independent Gaussian random variables with distribution

$$\begin{cases} \hat{r}_j \sim \mathbf{N}\left(N_sA_d^{(1)}\sqrt{E_g}, \sigma^2_{\mathrm{MAI}} + \frac{N_sN_0}{2}\right) & j = n \\ \hat{r}_j \sim \mathbf{N}\left(0, \sigma^2_{\mathrm{MAI}} + \frac{N_sN_0}{2}\right) & j \neq n \end{cases} \tag{43}$$

where $\sigma^2_{\mathrm{MAI}} = \zeta(N_sE_g(K-1)/\rho)$, $\zeta = 3\sqrt{\pi\lambda}/8$ for differentiated Gaussian pulses and $\zeta = 1/6$ for Manchester pulses. Note that σ^2_{MAI} increases with N_s, E_g, and the number of users K, and decreases with the spread ratio ρ.

Let $K = 1$ (single user case so that $\sigma^2_{\mathrm{MAI}} = 0$), then (43) can be rewritten after normalization by $\sqrt{N_s}$ as

$$\begin{cases} \hat{r}_j \sim \mathbf{N}\left(A_d^{(1)}\sqrt{N_sE_g}, \frac{N_0}{2}\right) & j = n \\ \hat{r}_j \sim \mathbf{N}\left(0, \frac{N_0}{2}\right) & j \neq n \end{cases}$$

which is equivalent to (11) noting that $E_s = N_sE_g$. This justifies the assumption of $N_s = 1$ for the analysis in the single user case.

B. Multiple-Access Capacity

From (43), we can conclude that the multiple-access BPPM UWB system has the same received vector representation as given in (4) for a single user BPPM UWB system

$$\mathbf{r} = \mathbf{s}_{mn} + \mathbf{w} \tag{44}$$

where $\mathbf{w}$ has zero mean and variance $\sigma^2 = \sigma^2_{\mathrm{MAI}} + (N_s/2)N_0$ in each real dimension. Thus the information theoretic capacity for a BPPM UWB system over AWGN with a single user given in (7) can be extended to the multiple-access case by substituting $\sigma^2_{\mathrm{MAI}} + (N_sN_0/2)$ for $\sigma^2 = (N_0/2)$, which gives (45), shown at the bottom of the page.

Applying the link budget model given in (8) under FCC Part 15 rules, the tradeoffs between number of users, reliable distance, system performance and channel capacity can be determined. Numerical results will be presented in Section V.

C. Multiple-Access Error Probability

Given the vector representation of the time-hopping multiple-access BPPM UWB system in (44), the error probability can be obtained from (13) by substituting $\sigma^2_{\mathrm{MAI}} + (N_sN_0/2)$ for $\sigma^2 = N_0/2$, giving

$$P_N = 1 - P_c \tag{46}$$

where

$$P_c = \int_0^{\infty}\left(\frac{1}{\sqrt{2\pi}}\int_{-r_1/\sqrt{\sigma^2_{\mathrm{MAI}}+(N_sN_0/2)}}^{r_1/\sqrt{\sigma^2_{\mathrm{MAI}}+(N_sN_0/2)}} e^{-x^2/2}dx\right)^{N/2-1} \times p(r_1)dr_1 \tag{47}$$

and

$$p(r_1) = \frac{1}{\sqrt{2\pi\left(\sigma^2_{\mathrm{MAI}} + \frac{N_sN_0}{2}\right)}}\exp\left(-\frac{(r_1 - N_s\sqrt{E_g})^2}{2\left(\sigma^2_{\mathrm{MAI}} + \frac{N_sN_0}{2}\right)}\right). \tag{48}$$

The upper bound for a single user BPPM system given in (22) can then be applied to (45) to obtain

$$\begin{aligned} P_N &< \left(\frac{N}{2} - 1\right)\frac{\sqrt{2}}{2}e^{-\left(N_s^2E_g/4\left(\sigma^2_{\mathrm{MAI}}+(N_sN_0/2)\right)\right)} \\ &\quad + e^{-\left(N_s^2E_g/2\left(\sigma^2_{\mathrm{MAI}}+(N_sN_0/2)\right)\right)} \\ &< Ne^{-\left(N_s^2E_g/2\left(\sigma^2_{\mathrm{MAI}}+(N_sN_0/2)\right)\right)} \end{aligned} \tag{49}$$

$$C = \log_2 N - \frac{1}{N}\sum_{m=1}^{2}\sum_{n=1}^{N/2} E_{r|s_{mn}} \times \left[\log_2\left(\sum_{p=1}^{2}\sum_{q=1}^{N/2}\exp\left(-\frac{r_n^2 - r_q^2 + \left(r_q - A_pN_s\sqrt{E_g}\right)^2 - \left(r_n - A_mN_s\sqrt{E_g}\right)^2}{2\left(\sigma^2_{\mathrm{MAI}} + \frac{N_sN_0}{2}\right)}\right)\right)\right] \text{ bits / channel use} \tag{45}$$

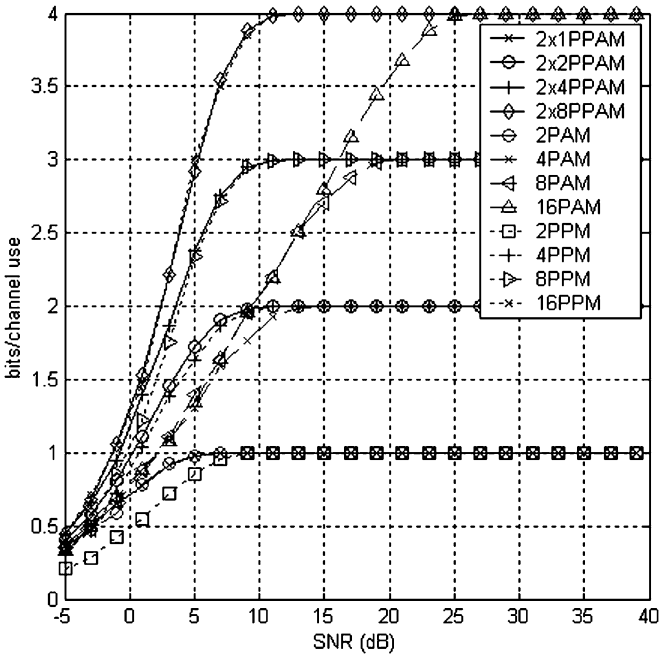

Fig. 2. Channel capacity with N-ary BPPM over an AWGN channel.

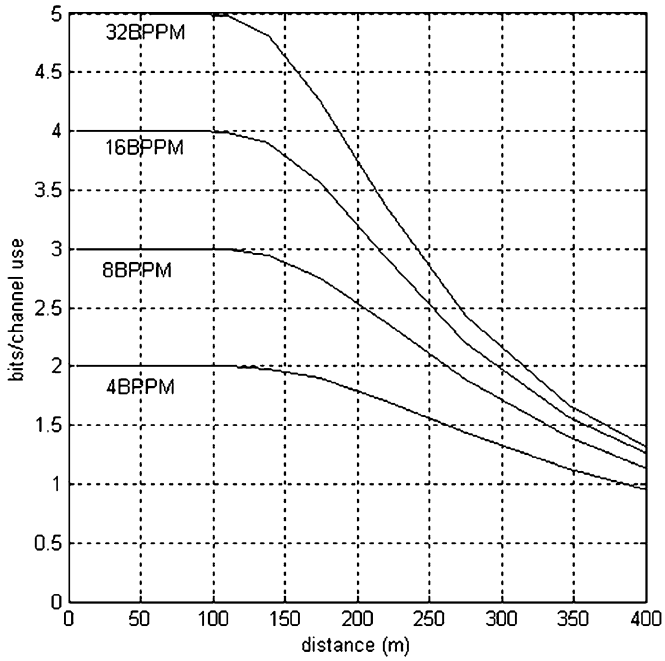

Fig. 3. UWB spectral efficiency as a function of range for $n = 2$, $G = 100$ and N-ary BPPM.

and similarly, (23) can be applied to give

$$P_{MN} < (N-1)Q\left(\sqrt{\frac{N_s^2 E_g}{2\left(\sigma_{\text{MAI}}^2 + \frac{N_s N_0}{2}\right)}}\right). \qquad (50)$$

V. Numerical Results

In this section, some numerical results are presented to illustrate and verify the capacity and error probability expressions obtained previously.

Fig. 2 shows the channel capacity for an N-ary BPPM system over an AWGN channel. This shows that N-ary BPPM has the same capacity as N-ary PPM and N-ary PAM for large SNRs. Note that 2-ary BPPM has almost the same capacity as 2-ary PAM, which can be justified by the fact that 2-ary BPPM is equivalent to 2-ary PAM. It is shown that 2-ary BPPM has a smaller SNR threshold to achieve capacity than 2-ary PPM. However, for N-ary BPPM, $N > 2$, the advantage over N-ary PPM decreases as N increases. This will also be shown by the performance of N-ary BPPM and N-ary PPM given later.

Fig. 3 illustrates the relationship between reliable channel capacity and communication range subject to FCC Part 15 rules. The link budget model in (8) was applied and a free space propagation transmission model was assumed, i.e., $n = 2$. The equivalent processing gain G was set to 100. This figure shows that N-ary BPPM can provide full capacity within 100 m in most cases, and approximately half of capacity when the communication distance is extended to 400 m for 4-ary BPPM.

The performance of 4-ary BPPM is shown in Fig. 4 for Gaussian first derivative pulses and Manchester pulses over an AWGN channel. The pulsewidth T_p was set to 0.6 ns in both cases, as well as the modulation index δ, and $N_s = 1$. The upper bounds given by (22) and (23) are also shown for comparison. The analytic (exact) error probability of (15) is included for reference. The two pulse types provide similar

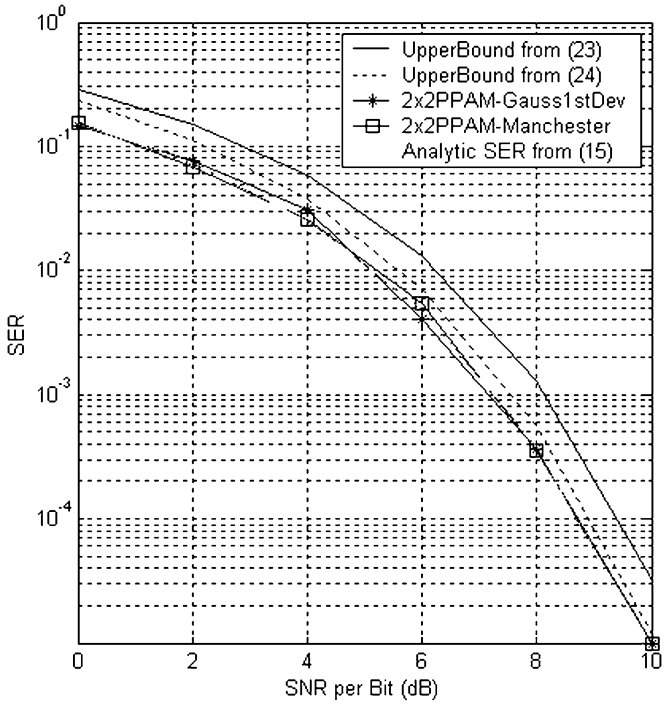

Fig. 4. Performance of a 4-ary BPPM UWB system with Gaussian first derivative pulses and Manchester pulses.

performance and match the exact SER, and (23) is a better bound than (22), and is sufficiently tight for large SNRs.

Fig. 5 compares the performance of BPPM, PAM, and PPM using Gaussian first derivative pulses. This shows that 4-ary BPPM has better performance than 2-ary PPM and 4-ary PPM, however, the advantage over 4-ary PPM is small, particularly for large SNRs, which follows from the similar SNR capacity thresholds in Fig. 2. Note that 4-ary BPPM has a computational

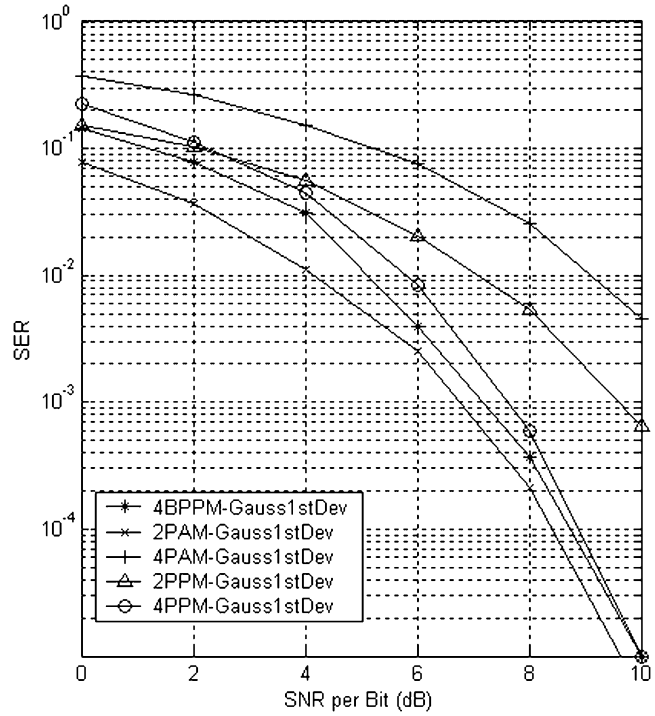

Fig. 5. Performance comparison between PAM, PPM, and BPPM with Gaussian first derivative pulses.

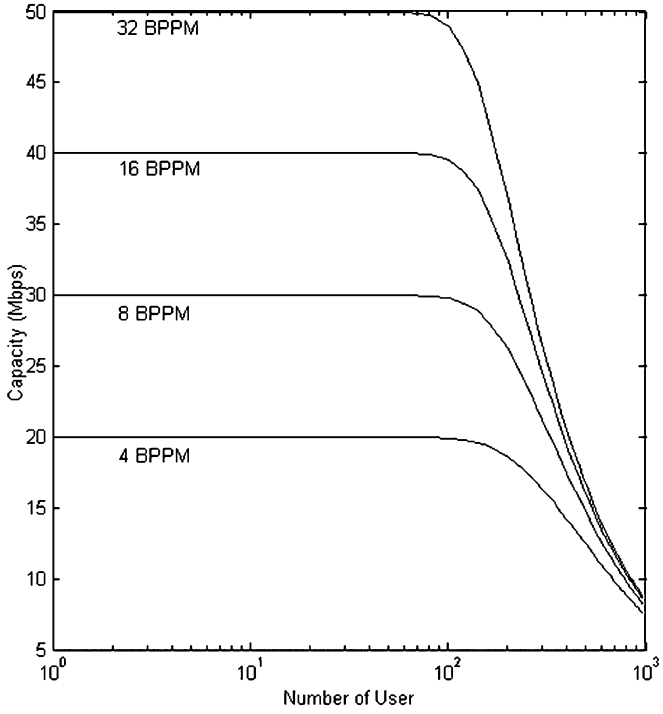

Fig. 7. Capacity of an N-ary BPPM UWB system with $\rho = 100$, $\mathrm{SNR} = 15$ dB, Manchester pulses and $Tp = 1$ ns.

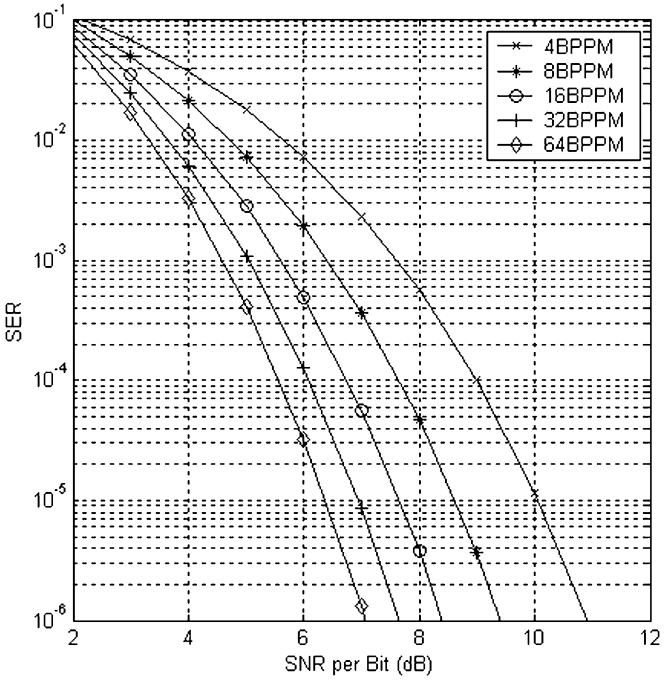

Fig. 6. Upper bound on error probability (24) for an N-ary BPPM UWB system.

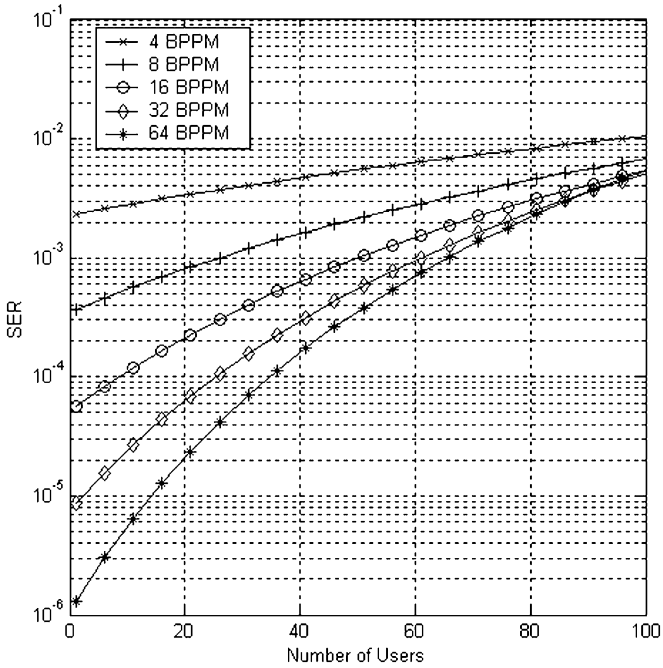

Fig. 8. Capacity of an N-ary BPPM UWB system with $\rho = 500, \mathrm{SNR/bit} = 7$ dB and Gaussian first derivative pulses.

complexity similar to 2-ary PPM with twice the capacity and better performance, while with the same capacity, it has only about half of the computational complexity of 4-ary PPM with better performance. Given this fact, 4-ary BPPM is an attractive choice for UWB communications.

Performance upper bounds are given in Fig. 6 for N-ary BPPM. This shows that better performance is achieved as N increases. However, the computational complexity doubles each time N increases by a power of 2, and the performance improvement diminishes.

User capacity in Mb/s is shown in Fig. 7 for $\mathrm{SNR} = 10$ dB, spread ratio $\rho = 100$, and Gaussian first derivative pulses with the pulsewidth set to 1 ns. The transmission rate, R_s, is given by $1/(\rho T_f)$. This shows that the system can accommodate approximately 100 simultaneous active users at full capacity. Only half

of the capacity can be achieved when the number of users is increased to 500 for 4-ary BPPM. With 15 users for 32-ary BPPM, 50 Mb/s can be achieved, while with 50 users, the achievable capacity is only 20 Mb/s.

Fig. 8 presents the user capacity from the perspective of error probability for a multiple-access time-hopping UWB system. Again N-ary BPPM is considered with an SNR per bit of 7 dB and a spread ratio of 500. This shows that the error probability increases as the number of users increases, as expected.

VI. Conclusion

A new modulation scheme, biorthogonal pulse position modulation, has been proposed for time-hopping UWB systems. The channel capacity and error probability have been analyzed over AWGN channels for both single and multiple user environments. It was shown that an N-ary BPPM UWB system provides better performance than an N-ary PPM system with only about half the computational complexity for the same thoughput. Thus, BPPM is an attractive alternative to PPM modulation for time-hopping UWB systems.

References

[1] R. A. Scholtz, "Multiple access with time-hopping impulse modulation," in *Proc. IEEE Military Commun. Conf.*, Oct. 1993, pp. 11–14.

[2] R. A. Scholtz and M. Z. Win, "Impulse radio," in *IEEE Int. Symp. Personal, Indoor and Mobile Radio Communication*, Sep. 1997, Invited Paper.

[3] L. Zhao and A. M. Haimovich, "Capacity of M-ary PPM ultra-wideband communications over AWGN channels," in *Proc. IEEE Vehicular Technology Conf.*, Oct. 2001, pp. 1191–1195.

[4] ——, "The capacity of an UWB multiple-access communications system," in *Proc. IEEE Int. Communications Conf.*, 2002, pp. 1964–1968.

[5] F. Ramirez-Mireles and R. A. Scholtz, "System performance analysis of impulse radio modulation," in *Proc. IEEE RAWCON*, Aug. 1998, pp. 67–70.

[6] ——, "Multiple-access performance limits with time hopping and pulse position modulation," in *Proc. IEEE Military Commun. Conf.*, Oct. 1998, pp. 529–533.

[7] J. R. Foerster, "The effects of multipath interference on the performance of UWB systems in an indoor wireless channel," in *Proc. IEEE Vehicular Technology Conf.*, May 2001, pp. 1176–1180.

[8] C. J. Le Marter and G. B. Giannakis, "All-digital PAM impulse radio for multiple-access through frequency-selective multipath," in *Proc. IEEE Global Telecommunications Conf.*, 2000, pp. 77–81.

[9] J. R. Foerster, "Ultra-wideband technology for short- or medium-range wireless communications," *Intel Tech. J.*, vol. Q2, pp. 1–11, 2001.

[10] M. Z. Win and R. A. Scholtz, "Ultra-wide bandwidth time-hopping spread-spectrum impulse radio for wireless multiple-access communications," *IEEE Trans. Commun*, vol. 48, no. 4, pp. 679–691, Apr. 2000.

[11] F. Ramirez-Mireles and R. A. Scholtz, "N-orthogonal time-shift-modulated codes for impulse radio," presented at the *IEEE Global Telecommun. Conf. Commun. Theory Mini Conf.*, Nov. 1997.

[12] O. Wintzell and D. K. Zigangirov, "On the capacity of a pulse-position-hopped CDMA system," *IEEE Trans. Inform. Theory*, vol. 47, pp. 2639–2644, Sep. 2001.

[13] F. Ramirez-Mireles and R. A. Scholtz, "Multiple-access with time hopping and block waveform PPM modulation," in *Proc. IEEE Int. Communications Conf.*, Jun. 1988, pp. 775–779.

[14] S. Verdú, "Recent progress in multiuser detection," in *Advances in Communications and Signal Processing*, W. Porter and S. Kak, Eds. Berlin, Germany: Springer-Verlag, 1989, vol. 129, pp. 27–38.

[15] G. Ungerboeck, "Channel coding with multilevel/phase signals," *IEEE Trans. Inform. Theory*, vol. 28, no. 1, pp. 55–67, Jan. 1982.

[16] J. G. Proakis, *Digital Communications*, 4th ed. New York: McGraw-Hill, 2001.

[17] R. E. Blahut, *Principles and Practice of Information Theory*. Reading, MA: Addison-Wesley, 1987, pp. 272–279.

[18] S. Dolinar, D. Divsalar, J. Hamkins, and F. Pollara, "Capacity of pulse-position modulation (PPM) on Gaussian and Webb channels," in *JPL TMO Progress Rep.*, vol. 42–142, Apr.–Jun. 2000, pp. 1–31.

[19] F. Ramirez-Mireles, "Ultra-wideband SSMA using time hopping and M-ary PPM," *IEEE J. Sel. Areas Commun.*, vol. 19, no. 3, pp. 1186–1197, Jun. 2001.

[20] G. Durisi and G. Romano, "On the validity of Gaussian approximation to characterize the multiuser capacity of UWB TH PPM," in *Proc. IEEE Conf. Ultra Wideband Systems and Technology*, 2002, pp. 157–161.

Hao Zhang was born in Jiangsu, China, in 1975. He recevied the B.S. degrees in telecom engineering and industrial management from Shanghai Jiaotong University, China, in 1994, the MBA from New York Institute of Technology, New York, in 2001, and the Ph.D. degree in electrical and computer engineering from the Univeristy of Victoria, Victoria, BC, Canada, in 2004.

From 1994 to 1997, he was the Assistant President of ICO (China) Global Communications Company. He was the Founder and CEO of Beijing Parco Company, Ltd. from 1998 to 2000. In 2000, he was a Software Engineer at Microsoft Canada and was Chief Engineer at Dream Access Information Technology, Canada, from 2001 to 2002. He is currently with the Department of Electrical and Computer Engineering, University of Victoria. His research interests include ultra wideband radio systems, MIMO wireless systems, and spectrum communications.

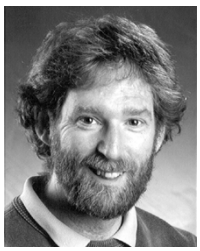

T. Aaron Gulliver (S'81–M'90–SM'96) received the B.S. and M.Sc. degrees in electrical engineering from the University of New Brunswick, Fredericton, NB, Canada, in 1982 and 1984, respectively, and the Ph.D. degree in electrical and computer engineering from the University of Victoria, Victoria, BC, Canada, in 1989.

From 1989 to 1991, he was a Defence Scientist at the Defence Research Establishment in Ottawa, Ottawa, ON, Canada, where he was primarily involved in research for secure frequency hop satellite communications. From 1990 to 1991, he was an Adjunct Research Professor in the Department of Systems and Computer Engineering, Carleton University, Ottawa. In 1991, he became an Assistant Professor and was promoted to Associate Professor in 1995. From 1996 to 1999, he was a Senior Lecturer in the Department of Electrical and Electronic Engineering, Univerity of Canterbury, Christchurch, New Zealand. Since July 1999, he has been an Associate Professor at the University of Victoria. His research interests include algebraic coding theory, cryptography, construction of optimal codes, turbo codes, spread spectrum communications, and the implementation of error control coding.

He is a member of the Association of Professional Engineer of Ontario, Canada.